JOURNAL OF BACTERIOLOGY, Dec. 2008, p. 7633–7644 Vol. 190, No. 23
0021-9193/08/$08.00+0 doi:10.1128/JB.01016-08

Regulation of Fatty Acid Metabolism by FadR Is Essential for *Vibrio vulnificus* To Cause Infection of Mice[▽]

Roslyn N. Brown and Paul A. Gulig*

Department of Molecular Genetics and Microbiology, University of Florida College of Medicine, P.O. Box 100266, Gainesville, Florida 32610-0266

Received 23 July 2008/Accepted 23 September 2008

The opportunistic bacterial pathogen *Vibrio vulnificus* causes severe wound infection and fatal septicemia. We used alkaline phosphatase insertion mutagenesis in a clinical isolate of *V. vulnificus* to find genes necessary for virulence, and we identified *fadR*, which encodes a regulator of fatty acid metabolism. The *fadR*::mini-Tn*5*Km2*phoA* mutant was highly attenuated in a subcutaneously inoculated iron dextran-treated mouse model of *V. vulnificus* disease, was hypersensitive to the fatty acid synthase inhibitor cerulenin, showed aberrant expression of fatty acid biosynthetic (*fab*) genes and fatty acid oxidative (*fad*) genes, produced smaller colonies on agar media, and grew slower in rich broth than did the wild-type parent. Deletion of *fadR* essentially recapitulated the phenotypes of the insertion mutant, and the Δ*fadR* mutation was complemented in *trans* with the wild-type gene. Further characterization of the Δ*fadR* mutant showed that it was not generally hypersensitive to envelope stresses but had decreased motility and showed an altered membrane lipid profile compared to that of the wild type. Supplementation of broth with the unsaturated fatty acid oleate restored wild-type growth in vitro, and infection with oleate in the inoculum increased the ability of the Δ*fadR* mutant to infect mice. We conclude that *fadR* and regulation of fatty acid metabolism are essential for *V. vulnificus* to be able to cause disease in mammalian hosts.

Vibrio vulnificus is a gram-negative opportunistic pathogen responsible for two serious diseases. Septicemia occurs after ingestion of raw, contaminated seafood in susceptible individuals, and wound infection occurs after contact with contaminated seawater or seafood products, leading to necrotizing fasciitis in otherwise healthy hosts (reviewed in reference 17). *V. vulnificus* infections are characterized by extremely rapid replication of the bacteria in the host and extensive tissue damage, with mortality rates as high as 75% and 50% for septicemia and wound infection, respectively (17). Although there are only about 50 confirmed cases of *V. vulnificus* infections annually in the United States (46), this bacterium has the potential for increased disease incidence during times of natural disasters. During hurricane Katrina in 2005, 14 cases of wound infection were attributed to *V. vulnificus*, and 3 resulted in death (4).

The means by which *V. vulnificus* causes such rapid, destructive, and lethal infection remain uncertain, despite a considerable amount of published research (17). The known virulence factors include the antiphagocytic capsule (43, 50, 51); iron sequestration via siderophores (28); flagella and motility (24, 26); type IV pili (36); the fibronectin-binding outer membrane protein OmpU (15); the HlyU protein, which upregulates expression of some toxin genes (22); and the RtxA1 toxin (23, 25, 29). Although some of the virulence factors discovered to date aid in growth and tissue damage, the levels of attenuation seen in these mutants vary, with some showing only marginal decreases in virulence. This led us to believe that important virulence factors remained to be discovered.

Our goal is to identify and characterize virulence factors of *V. vulnificus* that are involved with rapid growth, evasion of host defenses, and tissue damage. We used alkaline phosphatase (PhoA) mutagenesis (31) with a transposon-based delivery system for *phoA* based on mini-Tn*5*Km2 (7) (R. N. Brown and P. A. Gulig, unpublished results). PhoA mutagenesis takes advantage of the fact that the alkaline phosphatase enzyme is active only when transported outside the cytoplasm of a bacterial cell (19). A truncated *phoA* gene lacking a promoter and secretion signal sequence is randomly inserted into genes. An in-frame fusion of *'phoA* with a gene that encodes a secreted protein can be screened by using a chromogenic substrate for alkaline phosphatase, 5-bromo-4-chloro-3-indolyl phosphate (BCIP) (19). As part of our initial studies using PhoA mutagenesis, we obtained several mutants with decreased virulence (Brown and Gulig, unpublished). As described here, one of the insertions was in the *fadR* gene, encoding a regulator of fatty acid metabolism.

There is considerable published work on the roles of FadR in fatty acid metabolism and the glyoxylate shunt in *Escherichia coli*, but far less is known about FadR in other bacteria. The first reported role for FadR in *E. coli* was negative regulation of the fatty acid degradation (*fad*) genes (42). Nunn et al. (35) suggested a role for FadR in unsaturated fatty acid synthesis and noted that FabA enzyme (β-hydroxydecanoyl-thioester dehydrase) activity was decreased in the *fadR* mutant. Later, the *fabB* gene was also shown to be positively regulated by FadR in *E. coli* (3). *E. coli* FadR also activates *iclR*, encoding the repressor of the glyoxylate shunt enzymes (16), and represses *uspA*, encoding a universal stress protein (10). In *E. coli*, *fadR* mutants produce smaller amounts of unsaturated fatty acids

* Corresponding author. Mailing address: Department of Molecular Genetics and Microbiology, University of Florida College of Medicine, P.O. Box 100266, Gainesville, FL 32610-0266. Phone: (352) 392-0050. Fax: (352) 392-3133. E-mail: gulig@ufl.edu.

▽ Published ahead of print on 3 October 2008.

TABLE 1. Bacterial strains and plasmids

Strain or plasmid	Relevant characteristic(s)	Reference or source
Strains		
E. coli		
EC100D *pir*$^+$	F$^-$ *mcrA* Δ(*mrr-hsdRMS-mcrBC*) ϕ80d*lacZ*Δ*M15* Δ*lacX74 recA1 endA1 araD139* Δ(*ara*, *leu*)*7697 galU galK* λ$^-$ *rpsL* (Str^r) *nupG pir*$^+$(DHFR)	Epicentre
Top10	F$^-$ *mcrA* Δ(*mrr-hsdRMS-mcrBC*) ϕ80d*lacZ*ΔM15 Δ*lacX74 recA1 araD139*Δ(*ara-leu*)*7697 galU galK* λ$^-$ *rpsL* (Str^r) *endA1 nupG*	Invitrogen
S17-1λ*pir*	λ*pir thi pro hsdR hsdM*$^+$ *recA* RP4-2 Tc::Mu-Km::Tn*7*(Tp^r Sm^r)	41
V. vulnificus		
CMCP6	Clinical isolate	22
FLA399	Spontaneous rifampin-resistant derivative of CMCP6	This study
FLA602	FLA399 *fadR*::mini-Tn*5*Km2*phoA*	This study
FLA612	FLA602 reverted to *fadR*$^+$ by allelic exchange	This study
FLA614	CMCP6 Δ*fadR*::*aph*	This study
FLA1000	CMCP6 *ptsI*::mini-Tn*5*Km2*phoA*	F. Donoso and P. A. Gulig, unpublished results
Plasmids		
pCR2.1	T/A cloning vector; *lacZ*α multiple cloning site; Ap^r Km^r	Invitrogen
pCVD442	R6K *ori*-based suicide plasmid; *mob* RP4; *sacB*; Ap^r	9
pGTR201	pUTmini-Tn*5*Tag3*phoA* (*'phoA* delivery vector)	This study
pGTR349	*V. vulnificus fadR* cloned into pRK437 for complementation	This study
pGTR1129	pCVD442 with *lacZ*α from pUC19 with USER Friendly cloning oligonucleotide linker from pNEB206A (1); *cat*	Gulig et al., unpublished
pGTR2007	*fadR* cloned by USER into pGTR1129 for reversion	This study
pGTR2009	Sequences 500 bp upstream and 500 bp downstream flanking *fadR* cloned by USER into pGTR1129 for deletion of *fadR*	This study
pGTR2010	pGTR2009 with *aph* from pUC4K cloned between the *fadR* upstream and downstream sequences	This study
pRT291	IncP1; Tn*phoA*; Km^r Tc^r	48
pRK437	Expression vector; *mob* RK2; *lacZ*α multiple cloning site; Tc^r	40
pUC4K	Km^r derivative of pUC4	47
pUTmini-Tn*5*Tag3	Mini-Tn*5*Tag3 delivery vector; R6K *ori*; *mob* RP4; Ap^r Km^r	27

than do wild-type stains, but this was reported to be "phenotypically asymptomatic" (35). There have been no reports of FadR being essential for bacterial infection, and there is a scarcity of literature concerning the role of fatty acid metabolism during infection.

In the presently described work, we identified a transposon insertion in the *fadR* gene that did not result in an in-frame fusion to *'phoA* but greatly attenuated the ability of *V. vulnificus* to cause infection and death in iron dextran-treated mice. A *fadR* deletion was then constructed for better genetically controlled studies. The *fadR* mutants were defective in causing local skin lesions and lethal systemic liver infection compared with the wild-type parent. We also confirmed various FadR phenotypes in terms of altered gene expression, fatty acid composition, and sensitivity to certain drugs. We propose that FadR and proper coordination of fatty acid metabolism are important for the ability of *V. vulnificus* to establish lethal infection of mammalian hosts. These results could open the door for new avenues of antibacterial chemotherapy.

MATERIALS AND METHODS

Bacterial strains and media. The bacterial strains are listed in Table 1. *V. vulnificus* FLA399 is a spontaneous, rifampin-resistant derivative of clinical isolate CMCP6 (22). FLA602 is a mini-Tn*5*Km2*phoA* insertion mutant of FLA399 with the insertion in VV1_2233 (*fadR*), and FLA614 is CMCP6 Δ*fadR*::*aph*. *E. coli* Top10 (Invitrogen Corporation, Carlsbad, CA) was used for routine cloning procedures. TransforMax EC100D *pir*$^+$ electrocompetent *E. coli* (Epicentre Biotechnologies, Madison, WI) allowed for *lacZ*α complementation blue-white screening and maintenance of *pir*-dependent suicide plasmids. *E. coli* S17-1λ*pir* (41) was used as the donor strain for conjugations with *V. vulnificus*.

All strains were grown in Luria-Bertani broth containing 0.85% (wt/vol) NaCl (LB-N) or on LB-N plates containing 1.5% (wt/vol) agar. When required, antibiotics were used as follows: rifampin, kanamycin, chloramphenicol, and tetracycline at 50 μg/ml, 40 μg/ml, 30 μg/ml, and 12.5 μg/ml, respectively, for *E. coli* and 50 μg/ml, 300 μg/ml, 3 μg/ml, and 6.25 μg/ml, respectively, for *V. vulnificus*. Colistin (10^5 U/liter) was used to select against *E. coli* after conjugations. VVM (5), a selective and differential medium for *Vibrio* spp., was used to verify transconjugants as being *V. vulnificus*. M9 minimal salts (39) containing 0.2% (wt/vol) glucose or 0.01% (wt/vol) fatty acids was used to assess auxotrophy and the abilities of strains to use fatty acids as sole carbon sources.

Strains were stored at −80°C in LB-N with 35% (vol/vol) glycerol. For mouse infection experiments, static overnight starter cultures of bacteria were grown in culture tubes at room temperature. Before infection, starter cultures were diluted 1:20 into prewarmed LB-N and shaken at 37°C until the optical density at 600 nm (OD_{600}) reached 0.4 to 0.6 (exponential-phase growth). The bacteria were diluted in phosphate-buffered saline containing 0.01% (wt/vol) gelatin (BSG) (38) to the appropriate inoculum for infection. Further dilution in BSG and plating were used to confirm the number of CFU/ml inoculated.

Alkaline phosphatase mutagenesis and analysis of disease in mice. mini-Tn*5*Km2*phoA* (essentially a recreation of miniTn*5phoA* (7) was made by inserting *'phoA* from Tn*phoA* (31) into pUTmini-Tn*5*Tag3 (27) to form pGTR201 (Brown and Gulig, in preparation). *E. coli* S17-1λ*pir* carrying mini-Tn*5*Km2*phoA* on pGTR201 was conjugated with *V. vulnificus* FLA399 by filter mating. Transconjugants were selected on LB-N agar plates containing rifampin, kanamycin, 40 μg/ml BCIP (Sigma-Aldrich), and 0.2% (wt/vol) glucose. Glucose reduced the endogenous alkaline phosphatase activity of *V. vulnificus*, allowing for screening of PhoA$^+$ fusions on BCIP agar (50). Colonies appearing bluer than FLA399 on BCIP-containing plates were considered PhoA$^+$. The initial screen for virulence involved infection of two mice with each PhoA$^+$ mutant at

TABLE 2. Oligonucleotides used in this study

Oligonucleotide function and primer	Sequence (5′→3′)[a]
Cloning and deletion of genes	
TnPhoA5′-NotI-3	CGCGGCCGCCCTGTTCTGGAAAACCGGGCTGC
PhoA3′-NotI-2	GGCGGCCGCGGTTTTATTTCAGCCCCAGAGCGGC
vv12233-5′-rbs	CGGATCCTGAGTGCCATTCGACCCAAAAC
vv12233-3′	GGGATCCGTCAATTATTAGCTATTAGCAGTCG
FadR5′USER	**GGAGACAU**GACGACTTCCAGATTCCGCAA
FadR3′USER	**GGGAAAGU**CTATTAGCAGTCGTCTTCTGTG
sacB5′	AAGTTCCTGAATTCGATTCGTCC
sacB3′	CCTTTCGCTTGAGGTACAGCG
delfadRup5	**GGAGACAU**CTTGCCAAGTTACTTCCCTTGAA
delfadRup3	**ACCCGGGU**GGCTCTTTGCCTTAATGACCATT
delfadRdn5	**ACCCGGGU**AGACGACTGCTAATAGCTAATAATT
delfadRdn3	**GGGAAAGU**CCGATCCCGCGACCTTCTTG
DNA sequencing	
phoA5′-rev	CTGATCACCCGTTAAACG
qRT-PCR	
fabA Fwd	TTTGACTGCCATTTCCCTGG
fabA Rev	AACTGCCACATCGCATCCAA
fabB Fwd	TGTTTGCAGGTGGTGGTGAA
fabB Rev	TATTTGGTTGACAGTGCGCC
fadB Fwd	TCGTTGCTTACGCAGCCAAA
fadB Rev	AGCACGCGGTTCACAAAGAA
fadD Fwd	TGATGCCAAACCTGCTGCAA
fadD Rev	TCACAGCAATACAGCCAGCA
16S Fwd	TCGTCAGCTCGTGTTGTGAA
16S Rev	ACTCGCTGGCAAACAAGGAT

[a] Restriction sites are underlined, and USER cloning sequences are bolded.

an inoculum of 1,000 CFU (three times the wild-type minimum lethal dose). PhoA mutants that caused obvious signs of disease in mice (scruffy fur, lethargy, decreased body temperature, visible skin lesion upon necropsy) were considered virulent and were not studied further. Strains with decreased virulence compared to that of the wild type were examined by a repeat infection of five mice, followed by quantitative analysis of infection, described immediately below. Genomic DNA was extracted (DNeasy blood and tissue kit; Qiagen) from attenuated PhoA$^+$ strains for direct sequencing of the mutation by using oligonucleotide primer phoA5′-rev (Table 2) at the University of Florida Interdisciplinary Center for Biotechnology Research DNA Sequencing Core Laboratory.

Infection of mice. The subcutaneously (s.c.) inoculated, iron dextran-treated mouse model of Starks et al. (44, 45) was used. All animal experiments were approved by the University of Florida IACUC. Seven- to 10-week-old female ICR mice (Harlan Sprague-Dawley, Indianapolis, IN) housed under specific-pathogen-free conditions were used. Mice were injected intraperitoneally with 250 μg of iron dextran (Sigma-Aldrich) per gram of body weight at least 45 min before inoculation. Inocula consisting of 0.1 ml of bacteria suspended in BSG were injected s.c. in the lower back. In some experiments, as indicated, BSG was supplemented with 0.225% (wt/vol) sodium oleate. Mice were euthanized by carbon dioxide asphyxiation when rectal temperatures dropped below 33°C, indicating that mice were moribund, or at up to 22 h postinoculation.

After euthanization, the skin was peeled back to reveal the s.c. lesions. Samples of skin lesions and liver were aseptically removed from mice, homogenized in 5 ml of BSG by using glass tissue homogenizers, diluted, and plated on LB-N agar. For analysis of complementation of *V. vulnificus* FLA614 with pGTR349, samples were plated both nonselectively (LB-N) and selectively (LB-N with 6.25 μg/ml tetracycline). Samples were taken only from mice with visible skin lesions, and a minimum detectable number of CFU/g (10^4 CFU/g for skin and $10^{2.5}$ CFU/g for liver) was assigned for mice without lesions for statistical analysis.

Complementation of *fadR* mutations. The wild-type *fadR* gene, VV1_2233, was PCR amplified from *V. vulnificus* FLA399 genomic DNA by using the primers vv12233-5′-rbs and vv12233-3′ (Table 2) with *Taq* polymerase. The primers were designed to incorporate the putative *fadR* ribosome-binding site and to introduce flanking BamHI restriction sites for use in cloning. The 898-bp product was T/A cloned into pCR2.1-TOPO and electroporated into *E. coli* Top10 for *lacZ*α blue-white screening on LB-N plates containing tetracycline and 5-bromo-4-chloro-3-indolyl-β-D-galactopyranoside (X-Gal) (40 μg/ml). The VV1_2233 fragment was excised by BamHI digestion and cloned into the pRK437 cloning vector (40), digested with BamHI so that *fadR* could be expressed from the *lac* promoter. The complementing plasmid, pGTR349, was electroporated into *E. coli* S17-1λ*pir* for conjugation into *V. vulnificus* FLA602 and FLA614 by filter mating. Transconjugants were selected on LB-N plates containing kanamycin and tetracycline, and the presence of the plasmid was confirmed by agarose gel electrophoresis.

Construction of a *fadR*::mini-Tn*5*Km2*phoA* revertant. A genomic region of 1,009 nucleotides encompassing VV1_2233 was PCR amplified from *V. vulnificus* CMCP6 chromosomal DNA by using *Taq* polymerase and primers FadR5′USER and FadR3′USER to incorporate the USER sites. pGTR1129, a USER capture vector constructed using the allelic exchange vector pCVD442 (9) as a backbone, was used to clone the FadR-USER PCR product according to the USER Friendly cloning procedure (1) (New England Biolabs). DNA from the ligation reaction was purified using a DNA clean and concentrator kit (Zymo Research Corporation, Orange, CA) and electroporated into EC100D *pir*$^+$ for *lacZ*α blue-white screening on LB-N plates containing chloramphenicol and X-Gal. Plasmid mini-extracts of the resulting clones were resolved on an agarose gel to confirm the correct size. The insert of the reversion construct, pGTR2007, was sequenced to confirm the presence of the intact wild-type *fadR* gene. pGTR2007 was electroporated into *E. coli* S17-1λ*pir* for conjugation into *V. vulnificus* FLA602 by filter mating. Transconjugants were selected on LB-N plates containing chloramphenicol and colistin. Genomic DNA was tested by PCR using primers FadR5′USER and FadR3′USER to confirm the presence of the wild-type *fadR* gene and sacB5′and sacB3′ to confirm the integrated vector. After confirmation of plasmid integration, negative selection on LB-N agar plates containing 6% (wt/vol) sucrose was used to isolate cells that had undergone a second recombination event. This was confirmed by plating to observe chloramphenicol and kanamycin sensitivity and by PCR with primers FadR5′USER and FadR3′USER to show the presence of wild-type *fadR*, PhoA3′-NotI-2 and TnPhoA5′-NotI-3 to show loss of *′phoA*, and sacB5′ and sacB3′ to show loss of *sacB*. The resulting strain was named *V. vulnificus* FLA612.

Deletion of *fadR* from wild-type CMCP6. A three-part USER deletion method was used (P. A. Gulig et al., unpublished results). Briefly, 500-bp regions flanking VV1_2233 were PCR amplified using oligonucleotides delfadRup5/delfadRup3 and delfadRdn5/delfadRdn3. The upstream and downstream flanking DNA sequences were USER cloned into allelic exchange vector pGTR1129 (pCVD442::*lacZ*α::USER *cat*) (Gulig et al., unpublished), which was engineered to generate 3′ overhangs for capturing USER Friendly PCR amplicons, yielding pGTR2009. pGTR2009 was linearized by SmaI digestion and ligated with a blunt-ended *aph* (Kan^r) fragment from pUC4K (47), forming plasmid pGTR2010 carrying Δ*fadR*::*aph*. pGTR2010 was introduced into *V. vulnificus* CMCP6 by conjugation from *E. coli* S17-1λ*pir*, and a single crossover event was selected by resistance to chloramphenicol and kanamycin. After growth in the absence of chloramphenicol and the presence of kanamycin, double crossover events that replaced the wild-type *fadR* gene with the Δ*fadR*::*aph* allele were selected using sucrose resistance and chloramphenicol resistance. The proper allelic exchange event was confirmed by PCR, and the strain was named FLA614.

Growth rate. For measurement of growth rate in rich broth, static overnight cultures in LB-N were diluted 1:20 into prewarmed LB-N and grown with shaking at 37°C to exponential phase (OD_{600} = 0.4). Exponential-phase cultures were diluted to approximately 2.5×10^5 CFU/ml in 20 ml of LB-N or LB-N supplemented with 0.005% (wt/vol) sodium oleate and shaken at 37°C. Aliquots were removed for measurement of OD_{600} immediately and every 30 min thereafter for up to 5 h. To determine if strains could use glucose or fatty acids as a sole carbon source, static overnight cultures in M9-glucose were pelleted, washed once in M9 minimal salts without a carbon source, and suspended in 5 ml of M9, M9 plus 0.2% (wt/vol) glucose, M9 plus 0.01% (wt/vol) sodium decanoate (Sigma-Aldrich Inc.), or M9 plus 0.01% (wt/vol) sodium oleate (Sigma-Aldrich).

Turbidity after overnight incubation at room temperature indicated growth in the specified medium. Strains were also plated on LB-N agar to confirm viability.

Cerulenin MIC. A modification of the method of Campbell and Cronan (3) was used. Overnight cultures of *V. vulnificus* FLA602, CMCP6, and FLA602 (pGTR349) were diluted 1:200 into LB-N. Cerulenin (MP Biomedicals, Inc.) was dissolved in 100% (vol/vol) ethanol at 1 mg/ml and was added to culture tubes containing 1 ml of the diluted bacterial cultures to achieve concentrations of 20, 15, 10, 5, 2.5, 2, and 1 μg/ml. The tubes were incubated with shaking at 37°C overnight. The MIC was the concentration of cerulenin that resulted in no visible growth.

Quantitative reverse transcription-PCR (qRT-PCR) of FadR-regulated genes. A Qiagen RNeasy mini kit (Qiagen, Inc.) was used to isolate RNA from exponential-phase cultures (OD_{600} = 0.4 to 0.6) grown in LB-N. The RNA was treated with DNase I by using a Qiagen RNase-free DNase set during RNA extraction and was reverse transcribed using an iScript cDNA synthesis kit (Bio-Rad Laboratories, Inc.). To check for DNA contamination, purified RNA without reverse transcriptase was used as a negative control. A standard curve was plotted for each primer set by using known quantities of purified PCR products from CMCP6 genomic DNA. iQ Sybr green Supermix (Bio-Rad) was used for detection via the iQ real-time PCR detection system (Bio-Rad). The oligonucleotide primer sets are listed in Table 2. The PCR cycling conditions were 1 cycle at 95°C for 30 s, 40 cycles at 95°C for 10 s and 60°C for 45 s, 100 cycles at 60°C for 10 s, and a 4°C hold. The PCRs were done in triplicate. Relative expression levels were determined by the $2^{-\Delta\Delta Ct}$ method, using the 16S rRNA gene as an internal control. At least three separate experiments were performed for each gene.

Fatty acid analysis. Strains were grown to exponential phase (OD_{600} = 0.4 to 0.6) in LB-N at 37° with shaking. Cells were pelleted by centrifugation and used for fatty acid extraction, methyl esterification, and gas chromatographic analysis with the Sherlock system (MIDI Inc., Newark, DE) at the University of Florida Bacterial Identification & Fatty Acid Analysis Laboratory. Four independent experiments were done.

Assays of membrane stress sensitivity and motility. The MICs of ethanol, sodium dodecyl sulfate (SDS), and polymyxin B were determined essentially as done for cerulenin (described above). For ethanol, solutions of 6, 5, 4, 3, 2, and 1% (vol/vol) were made using 95% (vol/vol) ethanol in LB-N. The concentrations of SDS were 0.5, 0.45, 0.4, 0.35, 0.3, 0.25, 0.2, 0.15, and 0.1% (wt/vol) in LB-N. The polymyxin B concentrations were 350, 300, 250, 200, 150, and 100 U/ml in LB-N. For the assay of motility, static overnight cultures grown in LB-N at room temperature were stabbed in the centers of motility plates consisting of LB-N containing 0.3% (wt/vol) agar. Motility was measured as the diameter of spread after 15 to 17 h of incubation at 37°C.

Serum sensitivity assay. Static overnight starter cultures were diluted 1:20 in LB-N and grown to an OD_{600} of 0.4 to 0.6. Cultures were adjusted to 10^8 CFU/ml and serially diluted for plating to quantify input CFU. An aliquot of 20 μl from the 10^{-1} dilution (10^7 CFU/ml) was mixed and then incubated with 180 μl of untreated rat serum or heat-inactivated (30 min at 56°C) rat serum for 2 h at 37°C. The mixture was diluted and plated to quantify survival. The difference in log-transformed number of CFU between untreated and heat-inactivated sera was measured. Three independent assays were performed.

Statistical analyses. The Student *t* test was used to examine significant differences between pairs of means. Analysis of variance (ANOVA) with Bonferroni's posttest was used to identify significant differences when more than two pairs of means were analyzed. The χ^2 test was used in mouse experiments to determine if the number of mice with detectable CFU was significantly changed in mutant versus wild-type infections. *P* values of <0.05 were considered significant. Statistical analyses were done using Microsoft Excel or GraphPad Prism5 software. All quantitative experiments were repeated at least once.

RESULTS

A *V. vulnificus* mini-Tn*5*Km2*phoA* insertion mutant is severely attenuated for skin and liver infection in iron dextran-treated mice. Using methods detailed in Materials and Methods, we constructed a library of mini-Tn*5*Km2*phoA* insertions in *V. vulnificus* FLA399 to find mutants with decreased virulence in our mouse model of disease. Colonies that were bluer than the wild type on chromogenic BCIP agar plates were assumed to be $PhoA^+$ and were screened for virulence in mice. Colonies of *V. vulnificus* isolate FLA602 had a slightly bluer color than did the wild-type parent on BCIP plates. FLA602 also formed smaller colonies than did the wild type on LB-N agar plates and grew with a longer doubling time than did the wild type in LB-N (see below). However, the slow growth of FLA602 was not due to auxotrophy, since it could grow in M9 minimal medium. The initial screen for virulence involved s.c. inoculation of two iron dextran-treated mice with 1,000 CFU of *V. vulnificus* FLA602. In the initial screen and in three subsequent infections with inocula ranging from 2,000 to 4,000 CFU, *V. vulnificus* FLA602 failed to cause skin lesions in mice over a 22-h course of infection (data not shown). Mice inoculated with 300 CFU of wild-type *V. vulnificus* become moribund at 15 to 18 h postinfection. The FLA602-infected mice remained healthy in appearance, and the rectal temperatures were in the normal range for uninfected mice (37°C). To assess the extent of attenuation, we infected mice with increasing inocula of *V. vulnificus* FLA602. Inoculation of 10^4 CFU failed to cause skin lesions; the mice remained healthy in appearance, and body temperatures were similar to those for uninfected mice throughout the 22-h course of infection. Skin lesions were observed only with inocula at or above 10^5 CFU, and liver infection was detectable only at an inoculum of 10^7 CFU (Fig. 1). With an inoculum of 10^5 CFU of FLA602, only three of five mice had visible skin lesions and the mean number of bacteria recovered from the skin lesions ($10^{5.8}$ CFU/g skin tissue) was significantly lower than that for the wild type at an inoculum of 10^3 CFU (10^8 CFU/g skin tissue) ($P = 0.01$). Similarly, the number of bacteria recovered from liver samples of mice inoculated with 10^5 CFU of the mutant ($10^{2.4}$ CFU/g liver) was significantly lower than that for the wild type ($10^{4.7}$CFU/g) ($P = 0.0007$). Even when 10^6 CFU of the mutant was inoculated, levels of skin infection ($10^{6.1}$ CFU/g) and liver infection ($10^{2.5}$ CFU/g) were significantly lower than those for the wild type at a 10^3 CFU inoculum ($P = 0.04$ and $P = 0.0008$, respectively). An inoculum of 10^7 CFU of FLA602 resulted in wild-type levels of skin infection ($10^{7.8}$ CFU/g skin) but low levels of systemic infection ($10^{2.6}$ CFU/g; $P = 0.002$ for comparison to the wild type). FLA602 caused full wild-type levels of infection only when 10^8 CFU was inoculated. The mean temperatures of mice infected with 10^5, 10^6, or 10^7 CFU of FLA602 were also higher than those of mice inoculated with 10^3 CFU of the wild type. Additionally, the proportions of liver samples of mice that yielded bacteria from the mutant infections at 10^5, 10^6, and 10^7 CFU showed statistically significant decreases compared to the proportion of liver samples of mice that yielded bacteria from the wild-type infection ($P = 0.002$, $P = 0.002$, and $P = 0.04$, respectively; χ^2 test) (Fig. 1).

The FLA602 mini-Tn*5*Km2*phoA* insertion is in the *fadR* gene. The blue color of colonies of FLA602 on LB-N agar containing BCIP and glucose suggested that the mini-Tn*5*Km2*phoA* formed an in-frame gene fusion of a *V. vulnificus* gene to *'phoA*. However, DNA sequence analysis of genomic DNA from the mutant identified a backward insertion of *'phoA* into *V. vulnificus* CMCP6 gene VV1_2233, annotated as a "fatty acid metabolism regulator." PSORT (14) prediction based on the amino acid sequence suggested a cytoplasmic protein localization. The amino acid sequence contained the conserved domain FadR and had 52% identity to the well-studied *E. coli* FadR protein. As such, we named the mutated gene *fadR*. The mini-Tn*5*Km2*phoA* insertion occurred at nu-

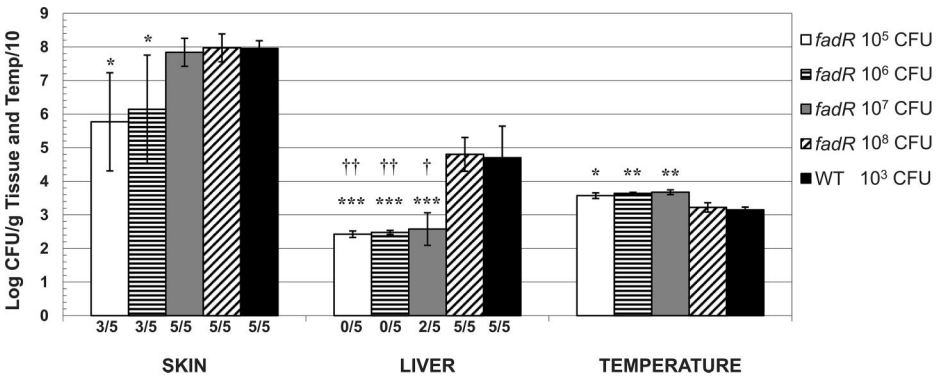

FIG. 1. Skin and liver infection caused by wild-type and *fadR V. vulnificus* in iron dextran-treated mice. Mice were inoculated s.c. with approximately 10^3 CFU of wild-type *V. vulnificus* FLA399 (WT) or 10^4, 10^5, 10^6, 10^7, or 10^8 CFU of *fadR*::mini-Tn*5*Km2*phoA* mutant FLA602. At up to 22 h postinfection, mice were euthanized, and skin and liver were sampled for quantification of *V. vulnificus*. Skin lesions were not observed with inocula of 10^4 CFU for the *fadR* mutant. Liver infection was detected only with an inoculum of 10^7 CFU. For samples with no detectable bacteria, the minimum detectable value was assigned for statistical analysis. Fractions beneath the bars indicate the numbers of mice that yielded detectable numbers of bacteria from the skin or liver samples over the number of inoculated mice. Asterisks indicate statistically significant differences in number of CFU/g tissue or temperature between mutant and wild-type infections (*, $P < 0.05$; **, $P \leq 0.01$; ***, $P \leq 0.001$; ANOVA with Bonferroni's posttest). Daggers indicate statistically significant differences in number of samples yielding bacteria between mutant and wild-type infections (†, $P = 0.04$; ††, $P = 0.002$; χ^2 test).

cleotide 346 of 840 in the *fadR* gene, meaning that the N-terminal 40% of the FadR protein was possibly translated.

Because FadR is a cytoplasmic protein, we were puzzled by the blue color of colonies of FLA602 on BCIP plates. We did not resolve the cause but noted that complementation and reversion of the mutation resulted in colonies that were similar in color to the wild type (see below), so the blue color of the *fadR*::mini-Tn*5*Km2*phoA* mutant on BCIP plates was not likely due to a secondary mutation. Furthermore, as detailed below, a Δ*fadR* mutation did not yield a similar blue color. Hence, the partially translated FadR protein of FLA602 might have caused the blue color.

Confirmation of the *fadR* phenotype. Although the gene interrupted by the mini-Tn*5*Km2*phoA* insertion possessed significant homology to *fadR* of *E. coli*, we further examined FLA602 to confirm the phenotype. The fatty acid synthase inhibitor cerulenin has been used as an indicator of the *fadR* mutant phenotype in *E. coli* (2, 3) and to inhibit fatty acid synthesis in *V. vulnificus* (6). Because FadR positively regulates genes involved in unsaturated fatty acid biosynthesis in *E. coli*, one aspect of the *fadR* mutant phenotype is decreased synthesis of unsaturated fatty acids (35). This renders the mutant hypersensitive to cerulenin because the drug further decreases fatty acid synthesis. Similar to *E. coli fadR* mutants, the *V. vulnificus fadR*::mini-Tn*5*Km2*phoA* mutant showed increased sensitivity to cerulenin compared to the level for the wild-type parent. The mutant had a mean MIC of 2.8 μg/ml cerulenin, in contrast to the wild-type parent, which had a mean MIC of 16.7 μg/ml, representing an approximately sixfold difference ($P = 0.001$; Student's *t* test). These values are the means for three biological replicates. This was similar to the 10-fold increase in sensitivity reported for an *E. coli fadR* mutant examined by Campbell and Cronan (3).

Increased cerulenin sensitivity in the *V. vulnificus fadR* mutant suggested decreased levels of the 3-ketoacyl-acyl carrier protein synthase I enzyme (FabB), the main target of the inhibitor (2, 37). To examine this possibility and to assess some aspects of FadR-regulated gene expression in FLA602, we performed qRT-PCR using genes known to be regulated by FadR in *E. coli*. In *E. coli*, FadR positively regulates at least two genes involved in unsaturated fatty acid biosynthesis, *fabA* and *fabB*, and negatively regulates genes involved in β oxidation (reviewed in reference 13). To determine if *V. vulnificus* FadR functioned similarly, we tested the relative expression levels of *fabA* and *fabB*, as well as two genes involved with β oxidation, *fadB* and *fadD*, in *fadR*::mini-Tn*5*Km2*phoA* mutant FLA602 and the wild type by using qRT-PCR. All gene expression levels were normalized to 16S rRNA levels as an endogenous control. Consistent with the expected results for a *fadR* mutation, the expression levels of *fabA* and *fabB* were lower and the *fadB* levels were higher than those of the wild type in FLA602. *fadD* expression was not significantly changed in FLA602 under the conditions tested (Table 3).

In vitro growth of *fadR*::mini-*Tn5*Km2*phoA* mutant FLA602. Increased sensitivity to cerulenin and changes in *fad* and *fab* gene expression suggested that the *fadR* mutant may be impaired for fatty acid metabolism. *E. coli fadR* mutants are able to grow using the medium-chain fatty acid decanoate as a sole carbon source, while wild-type cells cannot (20). In contrast,

TABLE 3. Expression of putative FadR-regulated genes in *V. vulnificus fadR*::mini-Tn*5*Km2*phoA* mutant FLA602[a]

Gene	Fold change (mean ± SD) in mutant	*P*
fabA	−8.4 ± 5.3	0.005
fabB	−6.9 ± 1.5	0.0002
fadD	−1.6 ± 2.1	0.1
fadB	4.2 ± 2.4	0.04

[a] FLA399 and FLA602 were grown to exponential phase in LB-N, and RNA was extracted. qRT-PCR was used to measure changes with the $2^{-\Delta\Delta Ct}$ method, using 16S rRNA as an endogenous control between *fadR* mutant FLA602 and wild-type FLA399. *P* values are for paired Student *t* tests comparing normalized threshold cycle values for the wild-type and mutant strains.

TABLE 4. In vitro growth rates and virulence levels of *V. vulnificus* strains

Strain	Genotype	Doubling time (min) in LB-N	Virulence[a]		
			Log no. of CFU/g		% of mice with detectable infection
			Skin	Liver	
FLA602	*fadR*::mini-Tn*5*Km2*phoA*	29	ND	ND	0[b]
FLA1000	*ptsI*::mini-Tn*5*Km2*phoA*	25	8.4 ± 0.2	6.3 ± 0.3	100
CMCP6	Wild type	18	8.5 ± 0.2	6.5 ± 1.5	100

[a] For virulence, five iron dextran-treated mice were inoculated s.c. with approximately 1,000 CFU, and infection was measured between 14 and 22 h later. ND, not detected.
[b] Compared with levels for FLA1000 and CMCP6 ($P = 0.002$; χ^2 test).

both wild-type and *fadR* mutant *E. coli* can use long-chain fatty acids, such as oleate, as carbon sources. We tested the growth of the *V. vulnificus fadR*::mini-Tn*5*Km2*phoA* mutant FLA602 and parental FLA399, using decanoate and oleate as sole carbon sources. Both *V. vulnificus* strains grew using both fatty acids as sole carbon sources. Unexpectedly, the *V. vulnificus fadR* mutant grew slower in rich LB-N than did the wild type (29-min versus 18-min doubling times, respectively) (Table 4), a phenotype that was not reported for *E. coli fadR* mutants. To test if the slow in vitro growth of FLA602 could be responsible for the observed decreased infectivity, we compared FLA602 with another slow-growing mutant generated by *phoA* mutagenesis, FLA1000, which contains a *ptsI*::mini-Tn*5*Km2*phoA* mutation. FLA1000 had a doubling time of 25 min in LB-N, compared to 18 min for the wild type; however, FLA1000 retained full virulence in mice (Table 4). Therefore, the slow in vitro growth of *fadR* FLA602 did not necessarily explain its severe attenuation in our mouse model of disease.

Complementation and reversion of the *fadR*::mini-Tn*5*Km2 *phoA* mutation. To prove that the attenuated infectivity phenotype of FLA602 was due to the knockout of the *fadR* gene by the transposon insertion and not a polar effect or secondary mutation, we introduced the wild-type *fadR* gene in *trans* into *V. vulnificus* FLA602 via plasmid pGTR349 (pRK437 containing the *V. vulnificus fadR* gene). Complementation of the *fadR*::mini-Tn*5*Km2*phoA* mutant restored the wild-type size to the colonies and reduced cerulenin sensitivity to wild-type levels (data not shown). The complemented strain looked identical to the wild type (pale blue) on BCIP plates, indicating that the blue color of FLA602 was somehow related to the genotype of *fadR*::mini-Tn*5*Km2*phoA*. Complementation also resulted in a significant increase in virulence (Fig. 2). At an inoculum of 1,000 CFU, skin lesions were observed in all mice ($P = 0.002$ for comparison to the *fadR*::mini-Tn*5*Km2*phoA* mutant; χ^2 test). These skin lesions yielded a mean of 7.7 ± 0.53 log CFU/g, similar to the level for a wild-type infection at this inoculum. Although high levels of skin infection were restored, liver CFU were detected in only one of five mice ($P = 0.29$ for comparison to the *fadR*::mini-Tn*5*Km2*phoA* mutant; χ^2 test). With an inoculum of 10^4 CFU, however, both skin and liver infections were detected at wild-type levels: 7.8 ± 0.28 log CFU/g skin and 4.8 ± 1.6 CFU/g liver.

Because complementation of the *fadR*::mini-Tn*5*Km2*phoA* mutant did not completely restore wild-type infection, we reverted the mutation by allelic exchange with the wild-type *fadR* gene. This would preclude the possibility of dominant-negative effects of the mutant FadR protein, in which the N-terminal 40% of the protein was intact. The truncated FadR protein would contain the critical N-terminal DNA-binding domain with residues that are predicted to form alpha helices that interact during dimerization and DNA binding (49). Thus, the truncated FadR protein could potentially dimerize with wild-

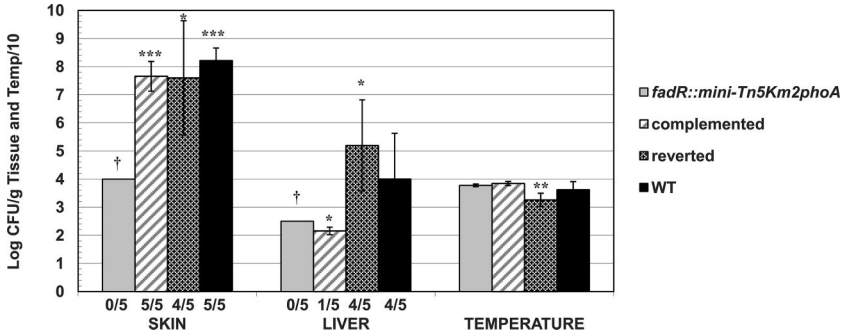

FIG. 2. Quantification of infection by *fadR*::mini-Tn*5*Km2*phoA* mutant FLA602 after complementation in *trans* with wild-type (WT) *fadR* or reversion by allelic exchange with wild-type *fadR*. Iron dextran-treated mice were infected s.c. with approximately 1,000 CFU of each *V. vulnificus* strain as detailed in Materials and Methods. Enumeration of the complemented strain on nonselective medium is shown. There was not a statistically significant difference between CFU counts on selective and nonselective media. Because the *fadR*::mini-Tn*5*Km2*phoA* strain was avirulent at this inoculum and did not yield CFU, the minimum detectable values for skin and liver, 10^4 and $10^{2.5}$ CFU/g, respectively, were assigned. Asterisks indicate statistically significant differences in number of CFU/g tissue or temperature between *fadR*::mini-Tn*5*Km2*phoA* infections and complemented, reverted, or wild-type infections (*, $P \leq 0.006$; **, $P \leq 0.001$; ***, $P \leq 3 \times 10^{-7}$; ANOVA with Bonferroni's posttest.) Daggers indicate statistically significant differences in number of samples yielding bacteria between the mutant skin infection and the complemented, reverted, or wild-type strain or between the mutant liver infection and the reverted or wild-type strain (†, $P \leq 0.01$; χ^2 test).

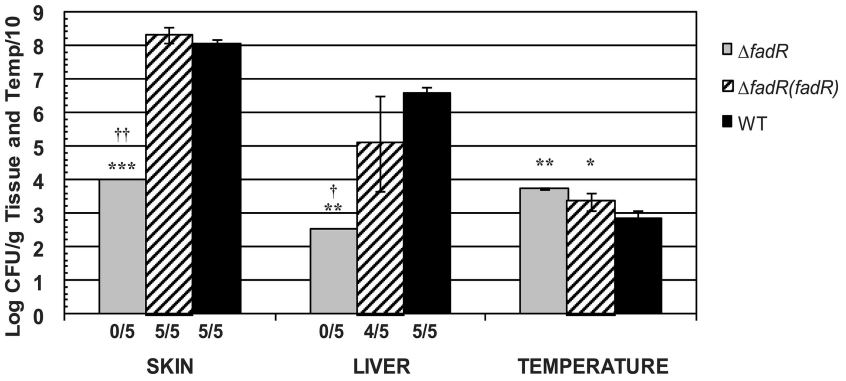

FIG. 3. Virulence of *V. vulnificus* Δ*fadR* and its complemented strain. Mice were inoculated with 1,000 CFU of Δ*fadR*::*aph* mutant FLA614 (Δ*fadR*), *fadR*-complemented strain FLA614(pGTR349) [Δ*fadR*(*fadR*)], or wild-type CMCP6 (WT). Enumeration of the complemented strain on nonselective medium is shown. There was not a statistically significant difference between CFU counts on selective and nonselective media. The Δ*fadR* strain was avirulent at 1,000 CFU and was assigned the minimum detectable values. The minimum detectable numbers of CFU for skin and liver samples are 10^4 and $10^{2.5}$ CFU/g, respectively. Fractions beneath the bars indicate the proportion of samples that yielded bacteria. Daggers indicate statistically significant differences in number of samples yielding bacteria between the mutant infection and the wild-type or complemented strain (†, $P \leq 0.01$; ††, $P = 0.002$; χ^2 test). Asterisks indicate significant differences in mean number of CFU/g tissue or temperature between the Δ*fadR* mutant and the wild-type or complemented strain (*, $P = 0.01$; **, $P = 4 \times 10^{-3}$; ***, $P \leq 2 \times 10^{-10}$; ANOVA with Bonferroni's posttest).

type FadR provided in *trans*, thereby reducing the efficiency of the complementation. In contrast to the complementation, reversion of the *fadR*::mini-Tn*5*Km2*phoA* mutation completely restored virulence in terms of skin and liver infection (Fig. 2). Mean bacterial yields from skin ($10^{7.6}$ CFU/g) and liver ($10^{5.2}$ CFU/g) tissues of infected mice were similar to those for the wild type ($10^{8.2}$ CFU/g skin and 10^4 CFU/g liver) at the same inoculum (1,000 CFU). Therefore, we concluded that the attenuated phenotypes of FLA602 were due to the *fadR* mutation.

Deletion of *fadR* from wild-type *V. vulnificus* CMCP6. To address the failure to fully complement the *fadR*::mini-Tn*5*Km2*phoA* mutation in *trans*, we deleted the *fadR* gene from wild-type *V. vulnificus* CMCP6, as described in Materials and Methods. The deletion mutant, FLA614, shared colony morphology characteristics with mini-Tn*5*Km2*phoA* insertion mutant FLA602; colonies were small and slightly yellow compared to those of the wild type. FLA614 also grew slower than the wild type in rich broth (discussed below; see Fig. 6) and was hypersensitive to cerulenin (not shown). Surprisingly, Δ*fadR* FLA614 did not appear bluer than the wild type on BCIP-containing media. This result suggested that the blue color seen for FLA602 was unique to the *fadR*::mini-Tn*5*Km2*phoA* mutation. Most notably, the deletion mutant was attenuated for infectivity in the mouse model of disease. At an inoculum of 1,000 CFU, FLA614 did not cause skin lesions and mice remained healthy throughout the 22-h course of infection (Fig. 3). Surprisingly, infections with increasing inocula showed that the deletion mutant was not as highly attenuated as the mini-Tn*5*Km2*phoA* insertion mutant, FLA602. An inoculum of 10^4 CFU of FLA614 was sufficient to cause skin lesions, although the level of skin infection ($10^{5.8}$ CFU/g) was more than 2 logs lower than the mean number of CFU/g recovered from an infection with the wild-type parent, CMCP6, at 1,000 CFU ($10^{8.4}$ CFU/g) ($P = 0.04$). Liver infection was detectable in only one of five mice inoculated with 10^4 CFU of FLA614 (mean, $10^{2.2}$ CFU/g liver). This value was also significantly lower than that for wild-type recovery ($10^{4.2}$ CFU/g liver) ($P = 0.003$), representing a 100-fold decrease in liver CFU for FLA614 with an inoculum that was 10-fold greater than that used for the wild-type infection. An inoculum of 10^6 CFU of FLA614 was sufficient to cause wild-type levels of skin and liver infection, with mean recoveries of $10^{8.3}$ CFU/g skin and $10^{5.6}$ CFU/g liver. Most importantly, complementation in *trans* with the *fadR* gene expressed from plasmid pGTR349 restored full wild-type virulence to Δ*fadR* FLA614. One thousand CFU of the complemented deletion strain caused wild-type levels of skin infection ($10^{8.3}$ CFU/g) and liver infection ($10^{5.1}$ CFU/g) in mice (Fig. 3). Because Δ*fadR* FLA614 was phenotypically similar to *fadR*::mini-Tn*5*Km2*phoA* FLA602 and was fully complemented in *trans*, we concluded that the *fadR* mutation was indeed responsible for the morphology, growth, and virulence phenotypes seen in both mutants, and FLA614 was used as a definitive *fadR* mutant for subsequent experiments.

Altered fatty acid content of *V. vulnificus* Δ*fadR*. Given that the *fadR* insertion or deletion mutations caused hypersensitivity to cerulenin and that decreased *fab* gene expression was evident, we hypothesized that a *fadR* mutant should exhibit decreased synthesis of unsaturated fatty acids that could lead to an altered membrane lipid profile (essentially all fatty acids and lipids in bacteria are found in the cell envelope [8]). Gas

TABLE 5. Changes in the fatty acid profile of *V. vulnificus* Δ*fadR* relative to that of the wild type[a]

Fatty acid type	Relative abundance (mean ± SD) in sample		% Change in mutant	*P*
	Wild type	Δ*fadR*		
Saturated	41.4 ± 1.9	46.9 ± 1.8	12	0.006
Unsaturated	57.8 ± 2.5	51.1 ± 1.8	−13	0.005

[a] Wild-type CMCP6 and Δ*fadR* mutant FLA614 were grown to exponential phase in rich broth, pelleted, and washed. Equal wet masses of cells of each strain were used for methyl esterification and gas chromatography-mass spectrometry. Relative abundance values are means ± standard deviations for four independent experiments. *P* values are for unpaired Student *t* tests comparing mutant and wild-type fatty acid abundance values.

TABLE 6. Sensitivities of wild-type and Δ*fadR V. vulnificus* strains to envelope stresses[a]

Envelope stress	MIC[b] (mean ± SD)		*P*
	Wild type	Δ*fadR*	
Ethanol	5 ± 0.8	4 ± 0.8	0.13
Polymyxin B	192 ± 38	217 ± 61	0.41
SDS	0.33 ± 0.06	0.22 ± 0.06	0.02

[a] Wild-type CMCP6 and Δ*fadR* mutant FLA614 were grown to exponential phase in rich broth. The MICs for ethanol, SDS, and polymyxin B were measured. Values are means ± standard deviations for at least four independent experiments. *P* values are for unpaired Student *t* tests comparing mutant and wild-type MICs. Except for a slight increase in sensitivity to SDS, the Δ*fadR* mutant was not more sensitive to envelope stresses than was the wild type.

[b] Values for ethanol are percentages (vol/vol), values for polymyxin B are numbers of U/ml, and values for SDS are percentages (wt/vol).

chromatographic analysis of fatty acid methyl esters derived from Δ*fadR* FLA614 and wild-type CMCP6 revealed a small (13%) but statistically significant ($P = 0.005$) decrease in unsaturated fatty acids and a concurrent 12% increase in saturated fatty acids in the Δ*fadR* mutant compared to the levels for the wild type ($P = 0.006$) (Table 5). Taken together, the increase in cerulenin sensitivity, the decrease in *V. vulnificus fab* gene expression, and the decrease in cellular unsaturated fatty acids suggested that *fadR* mutants are deficient in synthesis of unsaturated fatty acids.

Envelope stress sensitivity and motility of *V. vulnificus* Δ*fadR*. Because FLA614 showed slightly lower membrane unsaturated fatty acids than did the wild type, it was possible that the unbalanced fatty acid composition might render the mutant more susceptible to external stresses, possibly explaining the attenuated infection of mice. To test the susceptibility of the Δ*fadR* mutant to envelope stresses, we performed MIC experiments using chemicals that disrupt membrane integrity: ethanol, a membrane perturbant; SDS, a detergent that solubilizes the lipid bilayer; and polymyxin B, which binds lipopolysaccharide and disrupts membrane integrity. The MICs of ethanol and of polymyxin B for the Δ*fadR* mutant were similar to those for the wild type (Table 6). The Δ*fadR* mutant was slightly, but significantly, more sensitive to SDS than was the wild type, with 0. 22% (wt/vol) SDS causing growth inhibition of the mutant, compared to 0.33% for the wild type ($P = 0.02$) (Table 6). In light of the small magnitude of the change in SDS sensitivity and the fact that FLA614 was not hypersensitive to other membrane-perturbing agents, FLA614 was generally not more sensitive than the wild type to envelope stresses.

We also tested sensitivities to heat and cold as indications of membrane integrity. Δ*fadR* mutant FLA614 and wild-type CMCP6 were grown to exponential phase in LB-N, and serial dilutions were spotted onto LB-N plates and incubated at 37°C, 42°C, or 4°C for 18 h. FLA614 grew as well as CMCP6 at 37°C and 42°C (Fig. 4), but neither strain showed signs of growth after 18 h of incubation at 4°C (not shown). Further incubation of the 4°C plates overnight at room temperature (23°C) resulted in equal growth for both strains (Fig. 4). Overall, the Δ*fadR* mutant did not exhibit increased sensitivity to envelope stresses compared to that of the wild type.

As a further test of membrane defects, we tested the Δ*fadR* mutant for sensitivity to serum complement as an indicator of decreased resistance to host defenses. Δ*fadR* mutant FLA614, wild-type CMCP6, and complement-sensitive *E. coli* MG1655 bacteria were incubated in intact or heat-inactivated 90% rat serum for 2 h and then plated to quantify survival. *E. coli* MG1655 was completely killed by incubation with rat serum. The ratio of MG1655 bacteria that survived in untreated versus heat-inactivated sera was log -6.6 ± 0.4 ($P = 10^{-5}$ for comparison to *V. vulnificus* CMCP6; $n = 3$ biological replicates). In contrast, neither the Δ*fadR* mutant nor wild-type *V. vulnificus* was sensitive to complement-mediated killing. The ratio of CMCP6 bacteria that survived in untreated versus heat-inactivated sera was log 0 ± 0.1, and that for FLA614 was log -0.2 ± 0.2 ($P = 0.19$ for comparison to the wild type; $n = 3$ biological replicates). Because the Δ*fadR* mutant survived the bactericidal activity of serum complement as well as did the wild type, we concluded that the Δ*fadR* mutation did not cause a significant defect in the integrity of the cell envelope.

In addition to the possibility that loss of *fadR* could cause changes in envelope stress sensitivity, it was also possible that the Δ*fadR* mutant could be affected for motility. Motility is a complex function that requires the assembly and activity of the flagellum and motor apparatus across the cell envelope as well as ion gradients across the inner membrane to provide energy. Furthermore, flagella of the *Vibrionaceae* possess a sheath that appears to be an extension of the cell outer membrane (reviewed in reference 33). We therefore hypothesized that the altered fatty acid profile of the Δ*fadR* envelope could lead to changes in motility. We tested the motility of Δ*fadR* FLA614 and wild-type CMCP6 by measuring the diameter of spread through 0.3% motility agar. FLA614 was only 45% as motile as the wild type (Fig. 5) ($P = 3 \times 10^{-7}$). Motility was fully restored by complementation. We considered the possibility that the apparent decreased motility of Δ*fadR* FLA614 could have been due to its decreased growth rate. However, slow-growing *V. vulnificus* FLA1000 (Table 4) was fully motile compared to the wild type (data not shown).

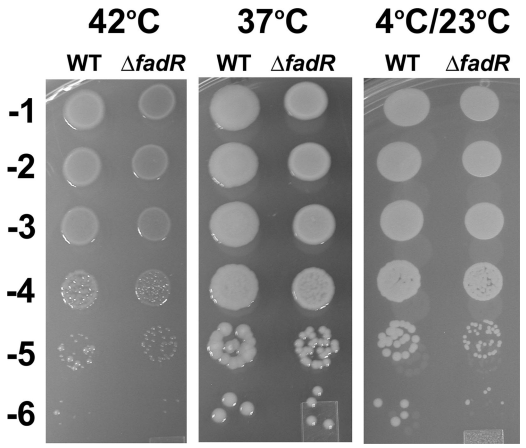

FIG. 4. Sensitivities of wild-type CMCP6 (WT) and Δ*fadR* FLA614 to heat and cold. Strains were grown to exponential phase at 37°C, and serial dilutions were aliquoted onto LB-N plates and incubated at the temperatures indicated for 18 h. The plates incubated at 4°C showed no visible growth after 18 h and were photographed after an additional overnight incubation at room temperature. Images are representative of triplicate plates. FLA614 was not more sensitive to heat or cold than was the wild type.

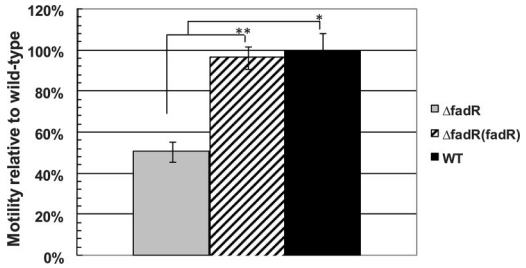

FIG. 5. Decreased motility of the Δ*fadR* mutant. Static overnight cultures of FLA614 (Δ*fadR*), complemented FLA614(pGTR349) [Δ*fadR*(*fadR*)], and wild-type CMCP6 (WT) were stabbed into the centers of 0.3% agar motility plates. The diameter of spread of bacteria was measured 15 h to 17 h later, and the mean for the wild type was assigned a value of 100%. Six plates per strain were used. At least two independent experiments were performed. Asterisks indicate significant differences between the Δ*fadR* mutant and the wild-type or complemented strain (*, $P = 3 \times 10^{-7}$; **, $P = 3 \times 10^{-8}$; ANOVA with Bonferroni's posttest).

Supplementation with unsaturated fatty acid in vitro and in vivo restores growth and infectivity. Deletion of *V. vulnificus fadR* resulted in a decreased growth rate in vitro and decreased levels of membrane unsaturated fatty acids. To test if the decreased in vitro growth rate of the *V. vulnificus* Δ*fadR* mutant was related to decreased unsaturated fatty acid synthesis, we supplemented LB-N with an unsaturated fatty acid derivative, sodium oleate, and measured the growth of Δ*fadR* FLA614 and wild-type CMCP6. The addition of 0.005% (wt/vol) sodium oleate (half the concentration used as a sole carbon source in M9 minimal medium) facilitated the growth of the Δ*fadR* mutant to wild-type levels (Fig. 6). Interestingly, wild-type CMCP6 did not grow any better when oleate was added to the growth medium, suggesting that the availability of fatty acids in LB-N was not a limiting factor for wild-type

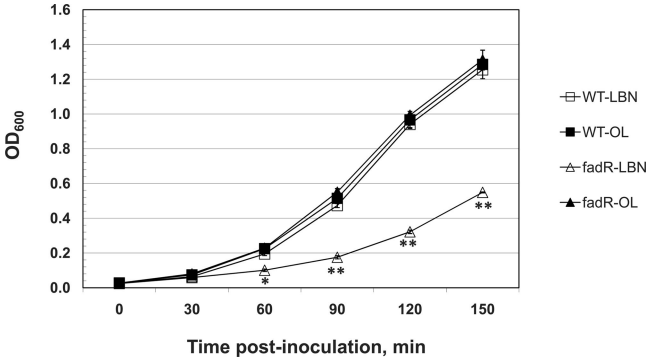

FIG. 6. Supplementation with oleate in vitro restores wild-type growth to *V. vulnificus* Δ*fadR* FLA614. A concentration of 2.5×10^5 CFU of wild-type CMCP6 or Δ*fadR* mutant FLA614 was inoculated into LB-N or LB-N plus 0.005% (wt/vol) sodium oleate and grown with shaking at 37°C. OD_{600} was measured every 30 min. Supplementation with oleate increased the growth rate and final yield of the Δ*fadR* mutant to wild-type levels. Data shown are means ± standard deviations for two independent experiments. Asterisks indicate significant differences between the Δ*fadR* mutant grown in LB-N (*fadR*-LBN) and the Δ*fadR* mutant grown with oleate (*fadR*-OL), the wild type grown in LB-N (WT-LBN), or the wild type grown with oleate (WT-OL) at each time-point (*, $P < 0.01$; **, $P < 0.001$; two-way ANOVA followed by Bonferroni's posttest).

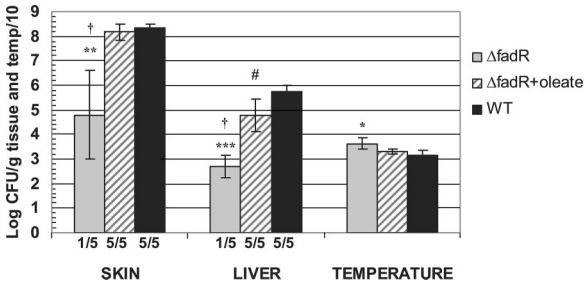

FIG. 7. Oleate potentiates infection of mice with Δ*fadR V. vulnificus*. Mice were inoculated s.c. with 1,000 CFU of Δ*fadR* mutant FLA614 suspended in BSG plus 0.225% (wt/vol) sodium oleate, FLA614 suspended in BSG alone, or wild-type CMCP6 (WT) suspended in BSG. Skin lesion and liver samples were plated to quantify infection. Daggers indicate statistically significant differences in number of samples yielding bacteria between the mutant infection and the oleate-supplemented mutant or the wild type ($P = 0.01$; χ^2 test). # indicates significant differences in number of CFU/g liver between oleate-supplemented Δ*fadR* and the WT ($P = 0.01$). Asterisks indicate significant differences in number of CFU/g tissue or temperature between the Δ*fadR* mutant and the wild type or oleate-supplemented Δ*fadR* (*, $P = 0.01$; **, $P \leq 0.003$; ***, $P \leq 3 \times 10^{-4}$; ANOVA with Bonferroni's posttest).

growth. The addition of 0.005% (wt/vol) sodium oleate to LB-N plates also significantly increased the mean diameter of colonies formed by the Δ*fadR* mutant. While the mean colony diameter of the Δ*fadR* mutant grown on LB-N plates was 2.4 ± 0.2 mm, the mean colony diameter for the mutant grown on LB-N plates supplemented with sodium oleate was 3.7 ± 0.4 mm ($P = 4 \times 10^{-4}$). Similar to the trend seen for wild-type CMCP6 grown in LB-N with oleate, the addition of oleate to LB-N plates did not significantly alter the mean colony diameter of wild-type CMCP6 (5.0 ± 0 mm on LB-N and 5.2 ± 0.4 mm on LB-N plus oleate; $P = 0.35$). Because supplementation with oleate functionally complemented the growth defect of the Δ*fadR* mutant in vitro, we inferred that the slow growth of the mutant in vitro was due to insufficient synthesis of unsaturated fatty acids.

To test if a relative lack of unsaturated fatty acids was responsible for the attenuation of the Δ*fadR* mutant, mice were infected with FLA614 suspended in sodium oleate or in BSG as a control. We used a concentration of sodium oleate (0.225% [wt/vol]) that was nearly 50-fold higher than that used for in vitro supplementation to compensate for equilibration with the fluid phase of the mouse. Mice were also infected with an equal inoculum of wild-type CMCP6 suspended in BSG for comparison. Control mice inoculated with sodium oleate alone showed no skin pathology upon necropsy (not shown). The addition of oleate to the inoculum allowed 1,000 CFU of the Δ*fadR* mutant to establish wild-type levels of skin infection ($10^{8.2}$ CFU/g skin tissue) and near-wild-type levels of systemic infection ($10^{4.8}$ CFU/g liver tissue), compared to what was found for CMCP6 ($10^{8.4}$ CFU/g skin [$P = 0.35$] and $10^{5.8}$ CFU/g liver [$P = 0.01$]) (Fig. 7). In contrast, the Δ*fadR* mutant without oleate supplementation established infection in only one of the five mice inoculated. Given that the oleate supplementation significantly increased the infectivity of the Δ*fadR* mutant in mice, we concluded that the major defect of the

Δ*fadR* mutant in vivo was insufficient synthesis of unsaturated fatty acids.

DISCUSSION

Identification of a *V. vulnificus fadR* mutation that is defective for infection of mice. We used alkaline phosphatase fusion-insertion mutagenesis to identify secreted virulence factors of *V. vulnificus* and isolated a mini-Tn*5*Km2*phoA* insertion in *fadR* (fatty acid metabolism regulator) that encodes a cytoplasmic protein. The transposon insertion was backward relative to the *fadR* open reading frame; hence, there was no *phoA* fusion. We do not understand the increased blue color of colonies of the *fadR*::mini-Tn*5*Km2*phoA* mutant on BCIP-containing agar plates, but it should be noted that, due to the presence of other alkaline phosphatase genes in the genome, *V. vulnificus* CMCP6 has a low level of background blue color on BCIP plates. Inclusion of glucose reduces the alkaline phosphatase activity but hinders growth. *fadR*::mini-Tn*5*Km2*phoA* FLA602 was one of the first mutants we isolated using PhoA mutagenesis; hence, it had no positive control for comparison. We subsequently used FLA602 as a negative control for blue color because it did not represent an in-frame *phoA* fusion. In any case, the *fadR*::mini-Tn*5*Km2*phoA* mutant was significantly attenuated for its ability to infect s.c. inoculated iron dextran-treated mice (Fig. 1), leading us to investigate the role of *fadR* and fatty acid metabolism in virulence of *V. vulnificus*. Part of this analysis included the construction of a *fadR* deletion mutant that generally exhibited the same phenotypes as the mini-Tn*5*Km2*phoA* mutant. The lack of blue color on BCIP plates and slightly milder attenuation of the deletion mutant suggested that the mini-Tn*5*Km2*phoA* mutation could have been polar on the downstream gene, *ribA*, encoding GTP cyclohydrolase II. However, *ribA* is 221 bp downstream, and there is a strong stem-loop structure resembling a transcriptional terminator immediately following *fadR*. In any case, we based our conclusions about *fadR* on the deletion mutant.

Comparison of *V. vulnificus* FadR with known FadR properties. Although the *V. vulnificus fadR* mutant was not a fatty acid auxotroph, it grew slower than did the wild type in rich LB-N (Table 4) and produced smaller colonies. These phenotypes were not reported for *E. coli fadR* strains (35), indicating that mutation of *fadR* in *V. vulnificus* has more severe phenotypic consequences. We confirmed expected *fadR* phenotypes, including cerulenin sensitivity and regulation of fatty acid-related genes (Table 3); moreover, the amplitudes of transcriptional regulation of *fab* and *fad* genes that we observed were within the range of those reported for *E. coli* (3, 10). Therefore, we are confident that our annotation of *fadR* to VV1_2233 is correct. Both *E. coli* and *V. vulnificus* wild-type strains grow using oleate as a sole carbon source, and *fadR* mutants of both species can grow using decanoate as a sole carbon source. However, wild-type *V. vulnificus*, but not wild-type *E. coli*, can grow using decanoate as a sole carbon source. A growth trend similar to that for *V. vulnificus* was reported for *Salmonella enterica* serovar Typhimurium (20). A recent study that compared various aspects of FadR proteins of several pathogens noted that the *Vibrio cholerae* FadR protein contains a 40-residue insertion relative to the *E. coli* protein (21). The amino acid sequence of *V. vulnificus* FadR is 85% identical to the *V. cholerae* sequence, and *V. vulnificus* FadR contains an identical 40-residue insertion relative to the *E. coli* protein. Because *V. vulnificus* FadR shares only 52% identity with the *E. coli* protein, there may be differences in protein function yet to be discovered.

Role of FadR in infection of mice by *V. vulnificus*. To our knowledge, the results reported herein are the first to demonstrate a role for *fadR* in the ability of a pathogen to infect animal hosts. Most of the literature on the role of fatty acid metabolism in bacterial virulence focuses on degradation (β oxidation). For example, *fadB* was identified in serovar Typhimurium as a gene specifically induced during infection (30). The authors suggested that fatty acid oxidation may be an important protective mechanism against proinflammatory and toxic host fatty acids. Fatty acid degradative defects are not likely the explanation for the attenuation of the *V. vulnificus fadR* mutant, as our results support previous reports that *fad* genes are expressed at higher levels in *fadR* mutants than in the wild type. To our knowledge, there has been no published work on the deleterious effects of constitutive fatty acid degradation during infection. Fatty acid synthesis was identified as important for acid tolerance and virulence of the cariogenic bacterium *Streptococcus mutans* (11, 12). A *fabM* (*trans*-2, *cis*-3-decenoyl-acyl carrier protein isomerase) mutant of *S. mutans* grew slower than did the wild type in vitro and had several altered enzymatic activities, including reduced glycolytic capability and altered glucose-phosphotransferase system activity (11). FabM in gram-positive bacteria functions similarly to FabA in gram-negative bacteria; both enzymes can isomerize the *trans*-2-enoyl bond of a nascent fatty acyl chain to the *cis*-3 isomer during fatty acid biosynthesis (reviewed in reference 32). This isomerization is essential for diversion of the growing acyl chain into the unsaturated fatty acid synthetic pathway. Therefore, loss of this isomerase activity results in decreased unsaturated fatty acid synthesis. Since a *V. vulnificus* Δ*fadR* mutant showed decreased expression of *fabA* (Table 3), we were not surprised that the mutant had some of the phenotypic characteristics reported for a *fabM* mutant (slow growth and decreased virulence). It remains to be seen if *V. vulnificus fadR* mutations also have the far-reaching enzymatic defects seen in the *S. mutans fabM* mutant.

We expected that a *fadR* mutation might severely impair membrane integrity and function, but we found that sensitivity to envelope stress was not increased in the Δ*fadR* mutant (Table 6 and Fig. 4) and that complement resistance was not impaired in the mutant. Therefore, it seemed that the altered membrane fatty acid profile of the Δ*fadR* mutant (Table 5) did not result in fragile membranes. On the other hand, the mutant was defective in motility (Fig. 5). The 55% decrease in the motility of the Δ*fadR* mutant compared to that of the wild type was similar to that seen in a *V. vulnificus* strain lacking the flagellin genes *flaCDE* (M. S. Tucker, P. C. Thiaville, and P. A. Gulig, unpublished results). This flagellar mutant showed decreased systemic infection but not decreased local infection. Even completely nonmotile *V. vulnificus* mutants (Δ*flaFBA*-Δ*flaCDE* and Δ*motAB*) retain the capacity to cause local infection (Tucker et al., unpublished), so the decrease in motility of the *fadR* mutant was not sufficient to explain the severe attenuation of infectivity.

While it can be argued that slow growth could contribute to

decreased virulence, we observed that another slow-growing mutant of *V. vulnificus* was capable of causing wild-type infection (Table 4). Therefore, slow growth in vitro is not necessarily a predictor of attenuated virulence. On the other hand, we noted that the growth rate of the *V. vulnificus* Δ*fadR* mutant could be functionally complemented in vitro by adding the fatty acid oleate to rich broth (Fig. 6), suggesting that the growth defect may be due to decreased unsaturated fatty acid synthesis. Likewise, inclusion of oleate in the inoculum caused a significant increase in skin infection during infection of mice (Fig. 7), indicating that a defect in fatty acid biosynthesis was the main factor causing decreased infectivity in the *V. vulnificus fadR* mutant.

During s.c. infection, wild-type *V. vulnificus* thrives in the host environment, with a doubling time of 15 to 28 min in iron dextran-treated mice (44, 45). We hypothesize that this bacterium, normally a resident of shellfish and estuarine water, causes lethal opportunistic infections in humans by overwhelming the host innate immune defenses by rapidly dividing to reach a critical mass while destroying host tissues with various toxins and enzymes. Our results reported here underscore the importance of FadR for regulating unsaturated fatty acid biosynthesis during the infectious process of *V. vulnificus*. These findings are likely to extend to additional bacterial pathogens. Because the bacterial fatty acid system differs from the mammalian system, this has long been an attractive target for antibiotics (reviewed in reference 18). However, some compounds identified for this purpose have had the drawback of interactions with the mammalian fatty acid metabolic system. For example, cerulenin interacts with mammalian fatty acid synthases (34). There is no FadR homolog in mammals. As such, FadR may be potential target for chemotherapy for *V. vulnificus* and other bacterial pathogens.

ACKNOWLEDGMENTS

This work was supported by NIH grant R01 AI056056.

We thank Jennifer Joseph, Patrick Thiaville, Julio Martin, and Aaron Mittel for assistance with animal experiments and Fernando Donoso for providing *V. vulnificus* FLA1000.

REFERENCES

1. **Bitinaite, J., M. Rubino, K. H. Varma, I. Schildkraut, R. Vaisvila, and R. Vaiskunaite.** 2007. USER friendly DNA engineering and cloning method by uracil excision. Nucleic Acids Res. **35:**1992–2002.
2. **Buttke, T. M., and L. O. Ingram.** 1978. Inhibition of unsaturated fatty acid synthesis in *Escherichia coli* by the antibiotic cerulenin. Biochemistry **17:** 5282–5286.
3. **Campbell, J. W., and J. E. Cronan, Jr.** 2001. *Escherichia coli* FadR positively regulates transcription of the *fabB* fatty acid biosynthetic gene. J. Bacteriol. **183:**5982–5990.
4. **Centers for Disease Control and Prevention.** 2005. Vibrio illnesses after Hurricane Katrina—multiple states, August-September 2005. MMWR Morb. Mortal. Wkly. Rep. **54:**928–931.
5. **Cerdà-Cuéllar, M., J. Jofre, and A. R. Blanch.** 2000. A selective medium and a specific probe for detection of *Vibrio vulnificus*. Appl. Environ. Microbiol. **66:**855–859.
6. **Day, A. P., and J. D. Oliver.** 2004. Changes in membrane fatty acid composition during entry of *Vibrio vulnificus* into the viable but nonculturable state. J. Microbiol. **42:**69–73.
7. **de Lorenzo, V., M. Herrero, U. Jakubzik, and K. N. Timmis.** 1990. Mini-Tn*5* transposon derivatives for insertion mutagenesis, promoter probing, and chromosomal insertion of cloned DNA in gram-negative eubacteria. J. Bacteriol. **172:**6568–6572.
8. **DiRusso, C. C., and T. Nystrom.** 1998. The fats of *Escherichia coli* during infancy and old age: regulation by global regulators, alarmones and lipid intermediates. Mol. Microbiol. **27:**1–8.
9. **Donnenberg, M. S., and J. B. Kaper.** 1991. Construction of an *eae* deletion mutant of enteropathogenic *Escherichia coli* by using a positive-selection suicide vector. Infect. Immun. **59:**4310–4317.
10. **Farewell, A., A. A. Diez, C. C. DiRusso, and T. Nystrom.** 1996. Role of the *Escherichia coli* FadR regulator in stasis survival and growth phase-dependent expression of the *uspA*, *fad*, and *fab* genes. J. Bacteriol. **178:**6443–6450.
11. **Fozo, E. M., and R. G. Quivey, Jr.** 2004. The *fabM* gene product of *Streptococcus mutans* is responsible for the synthesis of monounsaturated fatty acids and is necessary for survival at low pH. J. Bacteriol. **186:**4152–4158.
12. **Fozo, E. M., K. Scott-Anne, H. Koo, and R. G. Quivey, Jr.** 2007. Role of unsaturated fatty acid biosynthesis in virulence of *Streptococcus mutans*. Infect. Immun. **75:**1537–1539.
13. **Fujita, Y., H. Matsuoka, and K. Hirooka.** 2007. Regulation of fatty acid metabolism in bacteria. Mol. Microbiol. **66:**829–839.
14. **Gardy, J. L., C. Spencer, K. Wang, M. Ester, G. E. Tusnady, I. Simon, S. Hua, K. deFays, C. Lambert, K. Nakai, and F. S. Brinkman.** 2003. PSORT-B: improving protein subcellular localization prediction for Gram-negative bacteria. Nucleic Acids Res. **31:**3613–3617.
15. **Goo, S. Y., H. J. Lee, W. H. Kim, K. L. Han, D. K. Park, H. J. Lee, S. M. Kim, K. S. Kim, K. H. Lee, and S. J. Park.** 2006. Identification of OmpU of *Vibrio vulnificus* as a fibronectin-binding protein and its role in bacterial pathogenesis. Infect. Immun. **74:**5586–5594.
16. **Gui, L., A. Sunnarborg, and D. C. LaPorte.** 1996. Regulated expression of a repressor protein: FadR activates *iclR*. J. Bacteriol. **178:**4704–4709.
17. **Gulig, P. A., K. L. Bourdage, and A. M. Starks.** 2005. Molecular pathogenesis of *Vibrio vulnificus*. J. Microbiol. **43:**118–131.
18. **Heath, R. J., and C. O. Rock.** 2004. Fatty acid biosynthesis as a target for novel antibacterials. Curr. Opin. Investig. Drugs **5:**146–153.
19. **Hoffman, C. S., and A. Wright.** 1985. Fusions of secreted proteins to alkaline phosphatase: an approach for studying protein secretion. Proc. Natl. Acad. Sci. USA **82:**5107–5111.
20. **Iram, S. H., and J. E. Cronan.** 2006. The beta-oxidation systems of *Escherichia coli* and *Salmonella enterica* are not functionally equivalent. J. Bacteriol. **188:**599–608.
21. **Iram, S. H., and J. E. Cronan.** 2005. Unexpected functional diversity among FadR fatty acid transcriptional regulatory proteins. J. Biol. Chem. **280:** 32148–32156.
22. **Kim, Y. R., S. E. Lee, C. M. Kim, S. Y. Kim, E. K. Shin, D. H. Shin, S. S. Chung, H. E. Choy, A. Progulske-Fox, J. D. Hillman, M. Handfield, and J. H. Rhee.** 2003. Characterization and pathogenic significance of *Vibrio vulnificus* antigens preferentially expressed in septicemic patients. Infect. Immun. **71:** 5461–5471.
23. **Kim, Y. R., S. E. Lee, H. Kook, J. A. Yeom, H. S. Na, S. Y. Kim, S. S. Chung, H. E. Choy, and J. H. Rhee.** 2008. *Vibrio vulnificus* RTX toxin kills host cells only after contact of the bacteria with host cells. Cell. Microbiol. **10:**848–862.
24. **Kim, Y. R., and J. H. Rhee.** 2003. Flagellar basal body *flg* operon as a virulence determinant of *Vibrio vulnificus*. Biochem. Biophys. Res. Commun. **304:**405–410.
25. **Lee, J. H., M. W. Kim, B. S. Kim, S. M. Kim, B. C. Lee, T. S. Kim, and S. H. Choi.** 2007. Identification and characterization of the *Vibrio vulnificus rtxA* essential for cytotoxicity in vitro and virulence in mice. J. Microbiol. **45:**146–152.
26. **Lee, J. H., J. B. Rho, K. J. Park, C. B. Kim, Y. S. Han, S. H. Choi, K. H. Lee, and S. J. Park.** 2004. Role of flagellum and motility in pathogenesis of *Vibrio vulnificus*. Infect. Immun. **72:**4905–4910.
27. **Lehoux, D. E., F. Sanchagrin, and R. C. Levesque.** 1999. Defined oligonucleotide tag pools and PCR screening in signature-tagged mutagenesis of essential genes from bacteria. BioTechniques **26:**473–480.
28. **Litwin, C. M., T. W. Rayback, and J. Skinner.** 1996. Role of catechol siderophore synthesis in *Vibrio vulnificus* virulence. Infect. Immun. **64:**2834–2838.
29. **Liu, M., A. F. Alice, H. Naka, and J. H. Crosa.** 2007. The HlyU protein is a positive regulator of *rtxA1*, a gene responsible for cytotoxicity and virulence in the human pathogen *Vibrio vulnificus*. Infect. Immun. **75:**3282–3289.
30. **Mahan, M. J., J. W. Tobias, J. M. Slauch, P. C. Hanna, and R. J. Collier.** 1995. Antibiotic-based selection for bacterial genes that are specifically induced during infection of a host. Proc. Natl. Acad. Sci. USA **92:**669–673.
31. **Manoil, C., and J. Beckwith.** 1985. Tn*phoA*: a transposon probe for protein export signals. Proc. Natl. Acad. Sci. USA **82:**8129–8133.
32. **Marrakchi, H., Y. M. Zhang, and C. O. Rock.** 2002. Mechanistic diversity and regulation of Type II fatty acid synthesis. Biochem. Soc. Trans. **30:**1050–1055.
33. **McCarter, L. L.** 2001. Polar flagellar motility of the *Vibrionaceae*. Microbiol. Mol. Biol. Rev. **65:**445–462.
34. **Nomura, S., T. Horiuchi, S. Omura, and T. Hata.** 1972. The action mechanism of cerulenin. I. Effect of cerulenin on sterol and fatty acid biosynthesis in yeast. J. Biochem. **71:**783–796.
35. **Nunn, W. D., K. Giffin, D. Clark, and J. E. Cronan, Jr.** 1983. Role for *fadR* in unsaturated fatty acid biosynthesis in *Escherichia coli*. J. Bacteriol. **154:** 554–560.
36. **Paranjpye, R. N., and M. S. Strom.** 2005. A *Vibrio vulnificus* type IV pilin contributes to biofilm formation, adherence to epithelial cells, and virulence. Infect. Immun. **73:**1411–1422.

37. **Price, A. C., K. H. Choi, R. J. Heath, Z. Li, S. W. White, and C. O. Rock.** 2001. Inhibition of beta-ketoacyl-acyl carrier protein synthases by thiolactomycin and cerulenin. Structure and mechanism. J. Biol. Chem. **276:**6551–6559.
38. **Provence, D. L., and R. Curtiss III.** 1994. Gene transfer in gram-negative bacteria, p. 317–347. *In* P. Gerhardt, R. G. E. Murray, W. A. Wood, and N. R. Krieg (ed.), Methods for general and molecular bacteriology. American Society for Microbiology, Washington, DC.
39. **Sambrook, J., E. F. Fritsch, and T. Maniatis.** 1989. Molecular cloning: a laboratory manual. Cold Spring Harbor Laboratory Press, Cold Spring Harbor, NY.
40. **Scott, H. N., P. D. Laible, and D. K. Hanson.** 2003. Sequences of versatile broad-host-range vectors of the RK2 family. Plasmid **50:**74–79.
41. **Simon, R., U. Priefer, and A. Pühler.** 1983. A broad host range mobilization system for *in vivo* genetic engineering: transposon mutagenesis in gram negative bacteria. Bio/Technology **1:**784–791.
42. **Simons, R. W., P. A. Egan, H. T. Chute, and W. D. Nunn.** 1980. Regulation of fatty acid degradation in *Escherichia coli*: isolation and characterization of strains bearing insertion and temperature-sensitive mutations in gene *fadR*. J. Bacteriol. **142:**621–632.
43. **Simpson, L. M., V. K. White, S. F. Zane, and J. D. Oliver.** 1987. Correlation between virulence and colony morphology in *Vibrio vulnificus*. Infect. Immun. **55:**269–272.
44. **Starks, A. M., K. L. Bourdage, P. C. Thiaville, and P. A. Gulig.** 2006. Use of a marker plasmid to examine growth and death of *Vibrio vulnificus* in infected mice. Mol. Microbiol. **61:**310–323.
45. **Starks, A. M., T. R. Schoeb, M. L. Tamplin, S. Parveen, T. J. Doyle, P. E. Bomeisl, G. M. Escudero, and P. A. Gulig.** 2000. Pathogenesis of infection by clinical and environmental strains of *Vibrio vulnificus* in iron dextran-treated mice. Infect. Immun. **68:**5785–5793.
46. **Strom, M. S., and R. N. Paranjpye.** 2000. Epidemiology and pathogenesis of *Vibrio vulnificus*. Microbes Infect. **2:**177–188.
47. **Taylor, L. A., and R. E. Rose.** 1988. A correction in the nucleotide sequence of the Tn*903* kanamycin resistance determinant in pUC4K. Nucleic Acids Res. **16:**358.
48. **Taylor, R. K., C. Manoil, and J. J. Mekalanos.** 1989. Broad-host-range vectors for delivery of Tn*phoA*: use in genetic analysis of secreted virulence determinants of *Vibrio cholerae*. J. Bacteriol. **171:**1870–1878.
49. **van Aalten, D. M., C. C. DiRusso, J. Knudsen, and R. K. Wierenga.** 2000. Crystal structure of FadR, a fatty acid-responsive transcription factor with a novel acyl coenzyme A-binding fold. EMBO J. **19:**5167–5177.
50. **Wright, A. C., L. M. Simpson, J. D. Oliver, and J. G. Morris, Jr.** 1990. Phenotypic evaluation of acapsular transposon mutants of *Vibrio vulnificus*. Infect. Immun. **58:**1769–1773.
51. **Yoshida, S., M. Ogawa, and Y. Mizuguchi.** 1985. Relation of capsular materials and colony opacity to virulence of *Vibrio vulnificus*. Infect. Immun. **47:**446–451.